NUMERICAL INVESTIGATION ON THE EFFECTS OF SLOTTED HEIGHT ON PERFORMANCE OF LOUVER AND SLIT FINS AT DIFFERENT FIN PITCHES

Changshuang ZHI, Xusheng WANG, Yingwen LIU*

Key Laboratory of Thermo-Fluid Science and Engineering of MOE, School of Energy and Power Engineering, Xi'an Jiaotong University, Xi'an, Shaanxi 710049, PR China

* Corresponding author; E-mail: ywliu@xjtu.edu.cn

In this paper, the effects of slotted height at different fin pitches are analyzed in detail, aiming to investigate the function and optimal ratio of slotted height to fin pitch. In the cases of high Reynolds number for louver fin, the "bimodal phenomenon" of heat transfer coefficient begins to appear with the increasing slotted height. As the slotted height is about half of the fin pitch, the heat transfer coefficient has a local minimum value, of which there are two peaks on both sides. However, the pressure drop has been increasing with the increasing slotted height. The optimal slotted height under different fin pitches is more instructive than the optimal louver angle. For slit fin, the heat transfer coefficient increases first and then decreases with the increasing slotted height, so does the pressure drop. Meanwhile, as the slotted height is about 0.3~0.45 times and 0.5~0.65 times of fin pitch for louver fin and slit fin respectively, the comprehensive performance can reach a maximum. In general, louver fin has higher comprehensive performance than slit fin. However, for the fin pitch assigned to 1.8 mm and large slotted height, the louver fin has a comprehensive performance roughly similar to the slit fin.

Keywords: *Slit fin; Louver fin; Finned tube heat exchanger; Slotted height; Fin pitch; Air side performance*

1. Introduction

Finned tube heat exchanger is conspicuous in energy, refrigeration, automobile, microelectronics and other fields. Generally speaking, the finned tube exchanger is composed of round tube and plate fins. And the fluid in tube is water or refrigerant, the fluid on the fin side is air [1]. As the thermal resistance on the air side accounts for more than 85% [2], the configuration of plate fin is continuously optimized. Due to the geometric discontinuity, multiple fins can break and renew the boundary layer and enhance heat transfer [3-5]. Even though louver fin and slit fin are widely used and many researches have been done about the slotted height, there is no unified conclusion that can be generalized to conclude the optimal louver angle or slotted height for different fin pitches.

As far as the author knows, the earliest experimental research on louver fins was carried out by Kays and London [6], and the experimental methods and matters needing attention are summarized. Further, Kim and Bullard [7] found that fin pitch is independent of heat transfer coefficient, and pressure drop is negatively correlated with fin pitch by conducting an experimental study with the Reynolds number of 100~600. Qi et al. [8] concluded the contribution ratios of different factors by Taguchi methodology based on the database from Kim and Bullard [7], and believed that the ratio of

fin pitch to fin thickness is a very important factor. Hsieh and Jang [9] found the optimal parameter combination by Taguchi method, in which the fin pitch and louver angle are assigned to 2.1 mm and 36° respectively. Erbay et al. [10] conducted that the effects of fin pitch are greater than that of louver angle, and provided the optimal geometry at Re = 229 with the louver angle of 20°and fin pitch of 1.5 mm. Javaherdeh et al. [11] conducted the investigation for the different louver angles varying from 12° to 60° by ε-NTU method. The heat transfer rate can reach a maximum with the louver angle of 28°, and the proper louver angle stands in the region from 24° to 32°. Zuoqin et al. [12] provided an optimal value of 8 degrees for louver angle at a constant 2.06 mm fin pitch, and the comprehensive performance is improved by 19%. Sadeghianjahromi et al. [13] concluded that the j-factor first increases, then decreases, and finally increases as the angle increases for different fin pitches varying from 2.5 mm to 5.0 mm, and the optimal louver angle is about 20° according to the maximum j-factor and the minimum f-factor. It can be found that different studies have different evaluation criteria, and the traditional optimal angle cannot be extended to other occasions.

To the best of the author's knowledge, Nakayama and Xu [14] conducted the earliest experimental research on slit fin, and proposed the correlations according to the test results of three samples. However, Garimella et al. [15] believed that the above correlations from Nakayama and Xu[14] have a narrow application range. Further, Wang and Du [16-18] studied the effects of geometric factors and fitted the correlations. The above correlations can reflect the strong interaction for fin pitch and slotted height. Yun and Lee [19] established eighteen kinds of scaled-up models by Taguchi methodology, and considered that the fin pitch has the most effect on thermal hydraulic performance. Meanwhile, Wang et al. [20] concluded that the fin pitch has most significant effect on the thermal-hydraulic performance for the ring-bridge slit fin. Zhi et al. [21] conducted the numerical simulation on slit fin with small diameter at a constant slotted height, and considered that the largest contribution to j-factor is fin pitch and number of tube rows at low Re and high Re respectively. Further, Zhi et al. [22] independently studied the effects of slotted height and fin pitch, and provided the correlations. However, the function between fin pitch and slotted height has not been explored. Even though the longitudinal vortex generator has been put into research and application recently [23, 24], there is still no research indicating the function between fin pitch and slotted height.

It is well known that the optimal angle or slotted height is different under different fin pitches. This paper takes the slotted width as a fixed value, tries to define the slotted height of the louver fin according to the meaning of the slotted height of the slit fin, and explores the interaction function between the slotted height and the fin pitch, so as to find a proper ratio to guide the design of heat exchanger. Hence, a 3D numerical simulation is carried out to investigate the effects of slotted height at different fin pitches and different Reynolds numbers. Combined with the distributions of velocity, streamline and temperature, the variations of heat transfer coefficient and pressure drop with the slotted height are analyzed in detail under different fin pitches. Taking the maximum comprehensive performance as the objective, the function and optimal ratio of slotted height to fin pitch are obtained, which can provide theoretical support for engineering design.

2. Model description

2.1. Configuration and meshing

The configurations including louver fin and slit fin are presented in Fig. 1, in which the red point is the origin of the coordinate. The tube pitches in transverse and longitudinal are 13.5 mm and

13.56 mm respectively. The collar diameter is 5.19 mm, which is the sum of the tube outside diameter and twice fin thickness (δf). The slotted widths (Sw) in louver fin and silt fin are 1.3 mm and 1.2 mm respectively. This paper takes the slotted width as a fixed value, tries to define the slotted height of the louver fin according to the meaning of the slotted height of the slit fin, and explores the optimal proportion and interaction function between the slotted height and the fin pitch. The definitions in the slotted height (S_h) and fin pitch (Fp) can be seen in Detail A and Detail B.

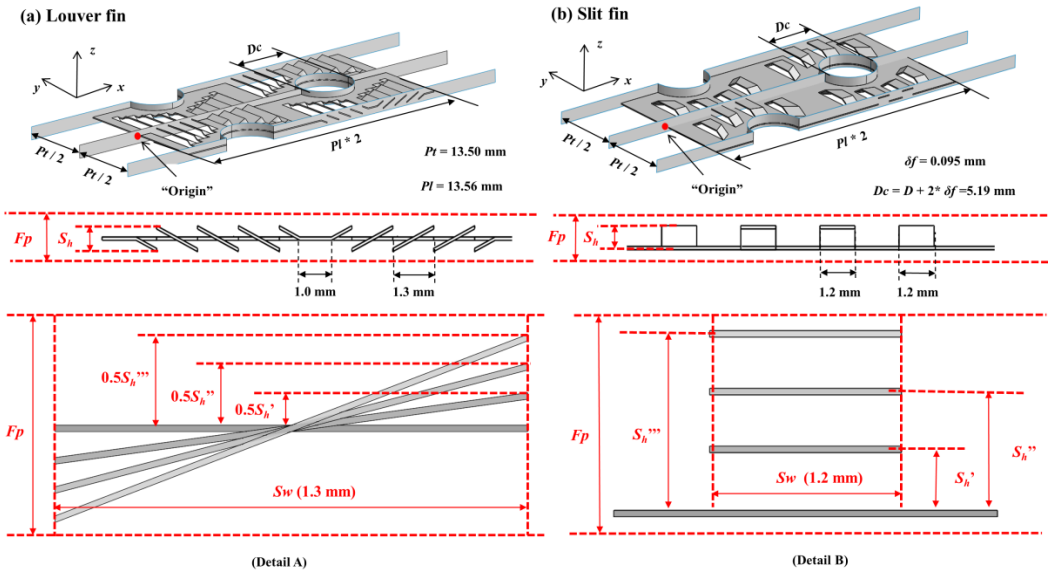

Figure 1. Configurations of the louver fin and slit fin in finned tube heat exchanger

The air in the domain flows along the x-axis direction, and symmetry and periodicity are assigned to the y-axis and z-axis respectively. In order to save computing consumption, the computational domain is defined as shown in Fig. 2, in which the height is a fin pitch and the length includes the louver/slit fin and the extensions. The minimal flow area will be generated between two adjacent tubes in the same row, and the flow velocity here is the maximum, as shown in Fig. 2. The upstream extension and downstream extension are 0.75 times and 4 times of the longitudinal tube pitch respectively, which can eliminate the effects of inlet and outlet. Table 1 exhibits the boundary conditions. The temperature of tube wall is 321.15 K, and the fin temperature is solved by conjugate [25-27], which is determined by the wall tube temperature and the air temperature. The inlet and outlet are set as the velocity inlet and pressure outlet respectively, and the air inlet temperature is 293.15 K, the velocity varies from 1.0 $m \cdot s^{-1}$ to 4.2 $m \cdot s^{-1}$. Li et al. [28] concluded that under different fluid physical properties, the Nusselt number and friction factor are almost the same at the same Reynolds number. It can be considered that the physical properties in the computational domain are constant. Hence, the physical properties in this paper are at the pressure of 0.101 MPa and temperature of 303.61 K, which are obtained by Refprop 9.1 as shown in Table 2.

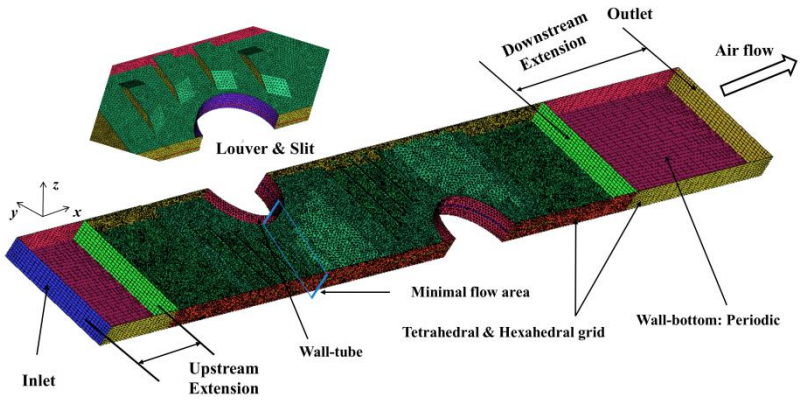

Figure 2. The computational domain and meshing

Table 1. Boundary conditions

u_{in} (m·s^{-1})	p_{outlet} (Pa)	T_{in} (K)	$T_{wall\text{-}tube}$ (K)	Wall-top&bottom	Wall-left&right
Velocity-inlet	Pressure-outlet				
1.0-4.2	0	293.15	321.15	Periodic	Symmetry

Table 2. The physical properties

Name	Density (ρ)	Specific heat (C_p)	Thermal conductivity (λ)	Dynamic viscosity (μ)
Unit	kg·m^{-3}	kJ·kg^{-1}·K^{-1}	W·m^{-1}·K^{-1}	Pa·s
Value	1.1589	1.0068	0.0263	1.8753×10^{-5}

The grid strategies around the tubes and fin surface can be presented in Fig. 2. Hexahedral grid is employed for upstream and downstream extensions, and tetrahedral grid is employed for fin coil area. It is necessary to have the grid independence for the better accuracy of the computations. The grid independence can be performed by the grid convergence index (GCI) method proposed by Roache [29], which is a method of minimizing the error of discrete equation solutions through grid refinement. Three sets of grids are assigned to the louver fin to eliminate the effect of grid density on numerical result as shown in Table 3, in which the slotted height (S_h) is 0.65 mm and the fin pitch (Fp) is 1.2 mm as a representative. The GCI for the three levels of grid refinements can be calculated by follows [30]. The f_i is the discrete solution under different grid strategies, including f_1, f_2 and f_3.

$$\mathrm{GCI}_{i+1,i} = \frac{Fs}{\left(r_{i+1,i}^{p}-1\right)}\left|\frac{f_{i+1}-f_i}{f_i}\right| \tag{1}$$

where Fs is the factor of safety, with a value of 1.25. The $r_{i+1,i}$ and p are the grid refinement ratio and order of accuracy respectively, which can estimated by follows.

$$r_{i+1,i} = \left(N_i / N_{i+1}\right)^{1/3} \tag{2}$$

$$\frac{f_3-f_2}{r_{3,2}^{p}-1} = \frac{r_{2,1}^{p}\left(f_2-f_1\right)}{r_{2,1}^{p}-1} \tag{3}$$

where N_i is the number of grids in the computational domain, including N_1, N_2 and N_3. Small value of

GCI indicates that the grids have achieved the convergence range, and the convergence range α of the solution should be close to 1, which can be calculated as follows [30].

$$\alpha = r_{2,1}^{p} \times \left(\frac{\mathrm{GCI}_{2,1}}{\mathrm{GCI}_{3,2}} \right) \tag{4}$$

Grid convergence calculations using GCI methods are carried out for all three levels of grid refinements are presented in Table 3. For all the variables, the value of p is always greater than 0, which indicates that the convergence condition is monotonic convergence [31]. Meanwhile, the value of α in all cases is very close to 1, which also indicates that monotonic convergence has been achieved. In addition, it can be found that the heat transfer coefficient and pressure drop have no obvious variety at all grid densities, and the errors are all at very low levels. Hence, in order to ensure the accuracy of the numerical model and save calculation consumption, the second grid density (846677) is selected as the final scheme.

Table 3. Verification of grid density independence

i	N_i	f_i	Error / %	$r_{i+1,i}$	f_{i+1}-f_i	$\mathrm{GCI}_{i+1,i}$	α	p
For Re = 600, h / W·m^{-2}·K^{-1}								
1	1490548	112.295	0.19%	1.073	0.216	0.005	1.002	6.032
2	1205219	112.511	0.57%	1.125	0.643	0.007		
3	846677	113.154						
For Re = 600, Δp / Pa								
1	1490548	28.090	0.47%	1.073	0.132	0.062	1.005	1.272
2	1205219	28.222	0.88%	1.125	0.247	0.068		
3	846677	28.470						
For Re = 2400, h / W·m^{-2}·K^{-1}								
1	1490548	186.861	0.5%	1.073	0.941	0.028	1.005	2.831
2	1205219	187.802	1.09%	1.125	2.049	0.034		
3	846677	189.851						
For Re = 2400, Δp / Pa								
1	1490548	228.202	0.37%	1.073	-0.834	0.050	0.996	1.238
2	1205219	227.368	0.69%	1.125	-1.559	0.055		
3	846677	225.809						

2.2. Data reduction

According to the conservation of heat transfer:

$$Q = c_p m\left(T_{out} - T_{in}\right) = h\left(A_{tube} + A_{fin} \cdot \eta\right)\Delta T_{log} \tag{5}$$

where ΔT_{log} is the logarithmic mean temperature difference and η is the fin efficiency, which can be

calculated as Eq.(6)-(7).

$$\Delta T_{\log} = \frac{\left(T_w - T_{in}\right) - \left(T_w - T_{out}\right)}{\ln \frac{T_w - T_{in}}{T_w - T_{out}}} = \frac{T_{out} - T_{in}}{\ln \frac{T_w - T_{in}}{T_w - T_{out}}} \tag{6}$$

$$\eta = Q / Q_{ideal} \tag{7}$$

where the Q_{ideal} is determined by $T_{fin}=T_{tube}$ in simulation.

Reynolds number, Nusselt number, Colburn factor-j, friction factor-f and performance evaluation criteria (*PEC*) are defined as follows [32].

$$Re = \frac{\rho u_{max} D_c}{\mu} \tag{8}$$

$$Nu = \frac{hD_c}{\lambda} \tag{9}$$

$$j = \frac{Nu}{Re\, Pr^{1/3}} \tag{10}$$

$$f = \frac{2\Delta p}{\rho u_{max}^2} \frac{A_c}{\left(A_{tube} + A_{fin}\right)} \tag{11}$$

$$PEC = j / f^{1/3} \tag{12}$$

where the u_{max} is the maximum velocity that can be calculated by conservation of mass, which is located at the minimum flow area in Fig. 2 [33].

2.3. Governing equations and model validation

Fluent 19.0 is employed to establish the numerical model. In this paper, the temperature and pressure are extracted from numerical simulation based on area-weighted average. The following is the continuity, momentum and energy governing equations. The flow is assumed to be incompressible with constant property and the air flow is steady. The viscous dissipation and gravity are neglected in this paper.

Continuity equation:
$$\frac{\partial\left(\rho u_i\right)}{\partial x_i} = 0 \tag{13}$$

Momentum equation:
$$\frac{\partial\left(\rho u_i u_k\right)}{\partial x_i} = \frac{\partial}{\partial x_i}\left(\mu \frac{\partial u_k}{\partial x_i}\right) - \frac{\partial p}{\partial x_k} \tag{14}$$

Energy equation:
$$\frac{\partial\left(\rho u_i T\right)}{\partial x_i} = \frac{\partial}{\partial x_i}\left(\frac{\lambda}{C_p}\frac{\partial T}{\partial x_i}\right) \tag{15}$$

The velocity and *Re* in this paper are low and the laminar model should be adopted to solve the numerical model. Meanwhile, the laminar model has been adopted in simulations of louver fin [34, 35] and slit fin [24]. The simulation results by laminar model are compared with the experimental correlations [16, 36], as shown in Fig. 3. The parameters for model validation are shown in Table 4. Although there are some inconsistencies between the parameter ranges in literature and the parameter

ranges in this study, the simulation model of the same size as that in literature is established and the calculations are carried out. For louver fin, the mean error of h is 2.94% and the mean error of Δp is only 1.32% within the entire velocity range. For slit fin, the mean error of h is 7.87% and the mean error of Δp is only 0.63% within the entire velocity range. The laminar model is consistent strongly with the experimental data within the entire velocity range, and the main errors come from the simplification of the numerical model. For example, a constant temperature is given to the wall tube in numerical simulation, which is only close to the constant in practice. In addition, there is no air passing through the symmetry, but it will occur in practice. Finally, convergence error of numerical simulation and measurement error of experiment will also contribute. Moreover, literature [34] summarized that even if it is noted that there is the error between CFD simulations and experimental results, the trend in CFD simulation is comparable.

Table 4. Parameters for model validation in literatures [16, 36]

Parameters	N	Pt	Pl	Fp	Ns	S_h	Sw	δ_f
Unit	-	mm	mm	mm	-	mm	mm	mm
Louver	1	25.4	19.05	1.915	6	0.9	2.4	0.115
Slit	2	25.4	22	2.48	4	0.99	2.2	0.12

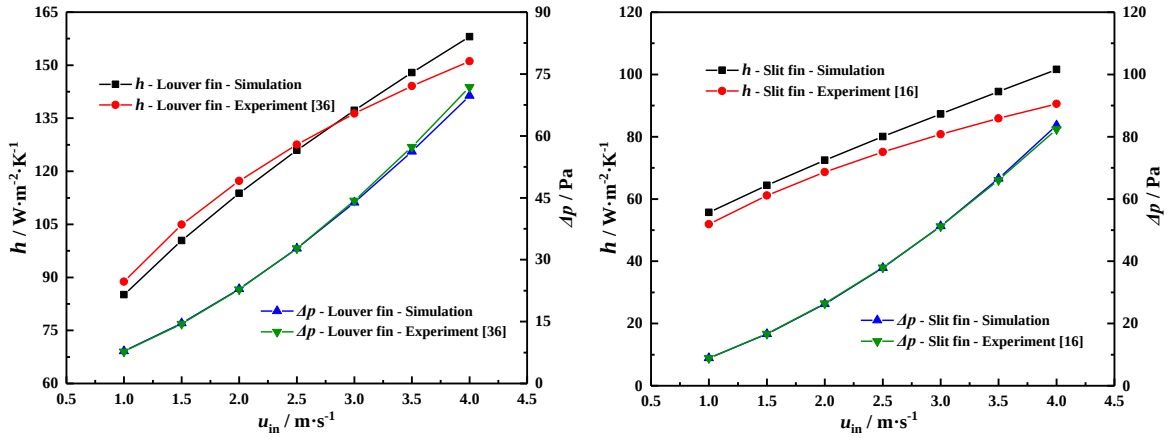

Figure 3. Comparison of h and Δp between the present and experimental data

3. Results and discussion

3.1. The effect of slotted height on louver fin performance

It can be observed from Fig. 4 that with the increasing S_h, the overall trend of the h at low Re is to increase first and then decrease. In the cases of high Re, the "bimodal phenomenon" begins to appear. As the S_h is about half of the F_p, the h has a local minimum value, of which there are two peaks on both sides. It can be mainly explained combined with the distributions of velocity and streamline at y = 0.2 mm. As the S_h is 0.25 mm (F_p = 1.2 mm) or 0.45 mm (F_p = 1.8 mm) shown in Fig. 5, the S_h is at a lower level than the F_p, and the air is directed by the fin (duct-directed flow) [10]. As the S_h continues to increase to 0.45 mm (F_p = 1.2 mm) or 0.775 mm (F_p = 1.8 mm), more air is directed by the louvers (louver-directed flow) [10], and the air passing between the two louvers of the upper layer can just scour the louvers of the lower layer, indicating that the h reaches the first peak (Peak-1). As the S_h is 0.65 mm (F_p = 1.2 mm) or 0.9 mm (F_p = 1.8 mm), the upper and lower louvers are

geometrically parallel shown in Fig. 5, which is falling under Scene-A explained in detail in Fig. 6. Further, the air passing through the upper louvers still passes through the lower louvers in parallel. Hence, the heat transfer coefficient has a local minimum. As the S_h continues to increase to 0.85 mm (F_p = 1.2 mm) or 1.25 mm (F_p = 1.8 mm), the geometric parallelism disappears. The air passing between the two louvers of the upper layer can scour the louvers of the lower layer again, and the h reaches the second peak (Peak-2). As the S_h continues to increase to 1.05 mm (F_p = 1.2 mm) or 1.65 mm (F_p = 1.8 mm), the upper and lower louvers are nearly completely parallel, and the h starts to decrease, which is falling under Scene-B explained in detail in Fig. 6. Fig. 7 shows the temperature distributions of louver fins at y = 0.2 mm. It can be clearly seen that the temperature distribution is roughly consistent with the distribution of heat transfer coefficient. There are still low temperature regions along the flow direction and the air cannot be effectively heated by the fins under duct-directed flow and Scene-B. The low temperature region under Scene-A is also slightly larger than the region at the Peak-1 and Peak-2. In addition, during the process of increasing the S_h, the Δp has been increasing. It can be interpreted as that with the increasing S_h, the Δp caused by changing of the flow direction plays a decisive role. It can be seen from Fig. 5 that for all cases where the fin pitch is 1.2 mm, the streamline is smooth and there are no vortices present. For the cases where the fin pitch is 1.8 mm, the streamline is also smooth if the slotted height is less than 0.9mm. As the slotted height increases to 1.25 mm, a part of the vortex can be clearly seen in the blue box, as shown in Fig. 5. Hence, it can be concluded that vortices appear at the larger slotted height and fin pitch, which is easy to cause greater pressure drop shown in Fig. 5. According to the geometric relationship, it can be found that the optimal slotted height under different fin pitches is more instructive than the optimal louver angle.

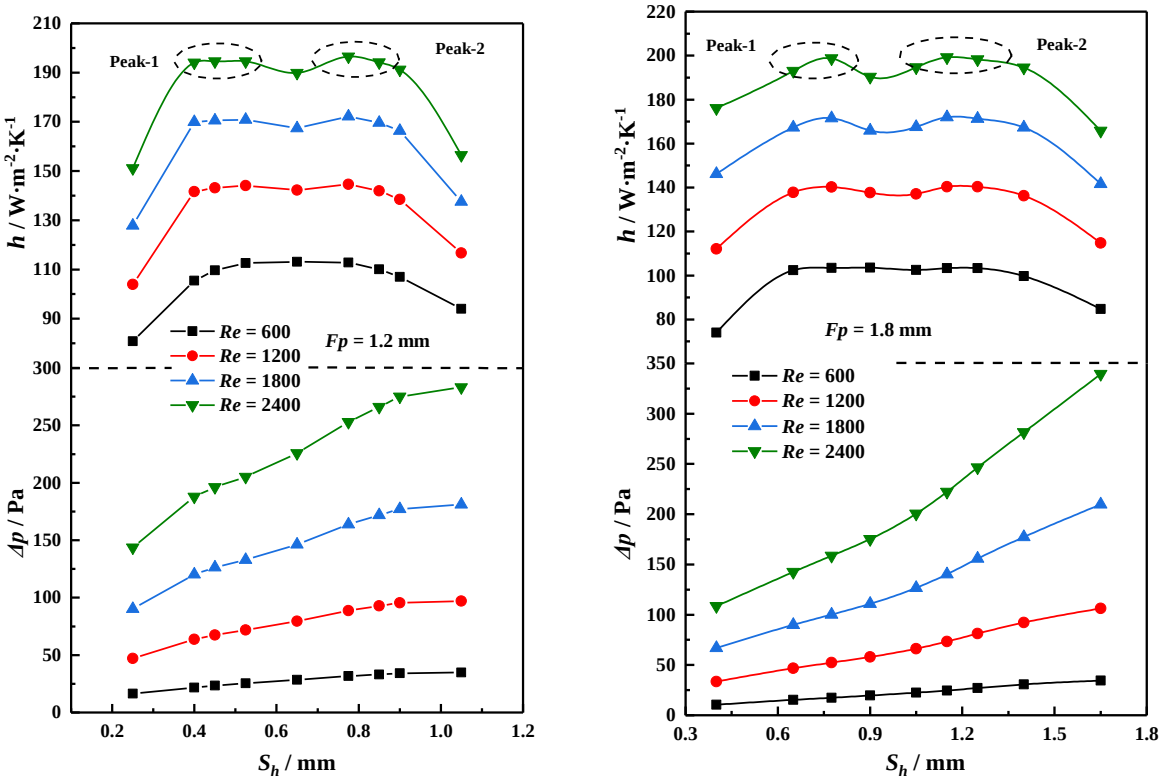

(a) Fp = 1.2 mm *(b) Fp = 1.8 mm*

Figure 4. Effects of slotted height on *h* and *Δp* at different fin pitches for louver fin

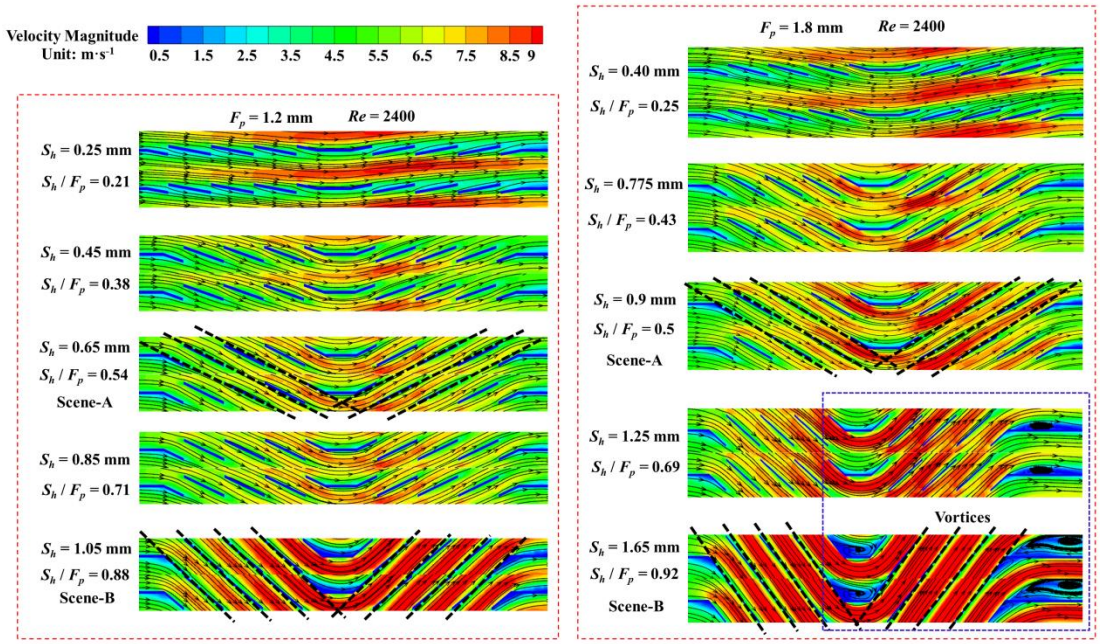

Figure 5. Contours of velocity and streamline at different slotted heights (y = 0.2 mm)

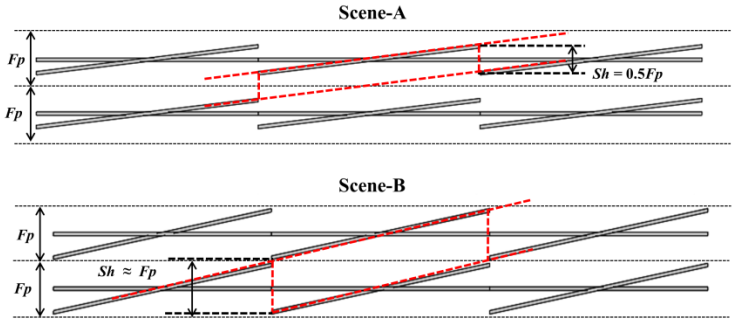

Figure 6. The scenes where the upper louver is parallel to the lower louver

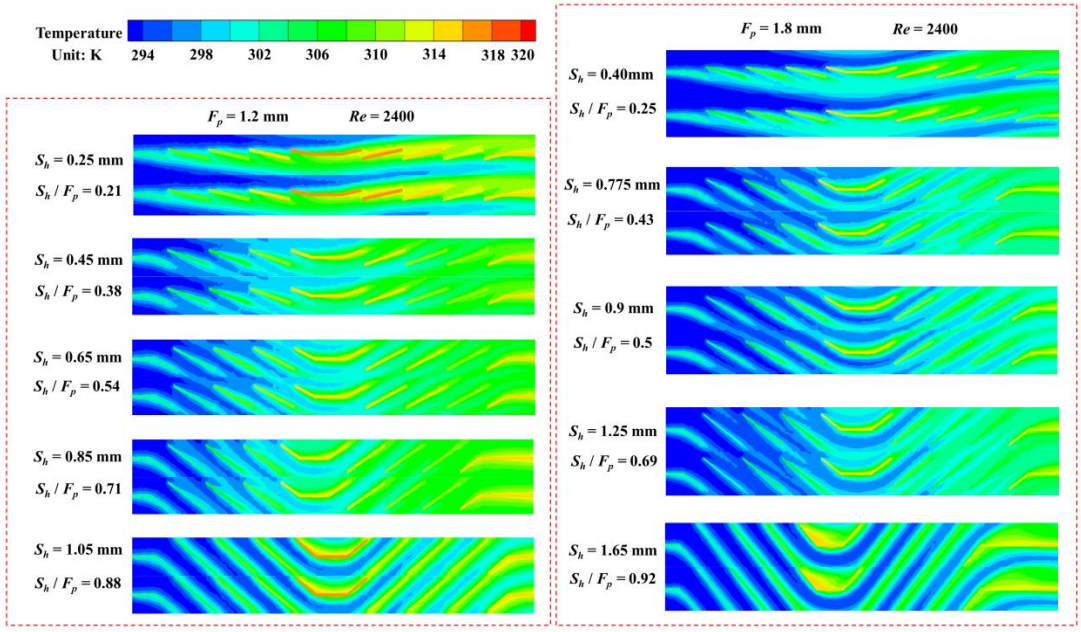

Figure 7. Contours of temperature at different slotted heights and fin pitches (y = 0.2 mm)

3.2 The effect of slotted height on slit fin performance

Fig. 8 outlines the varieties of the h and Δp under different slotted heights and fin pitches. The h and Δp increase first and then decrease with the increasing slotted height. As the slotted height is half of the fin pitch, the h and Δp can reach the maximum. And with the increase of Reynolds number, the slotted height corresponding to the maximum value increases. According to the contours of streamline and velocity at y = 2 mm in Fig. 9, it can be interpreted as follows. As the slotted height is 0.25 mm (F_p = 1.2 mm and F_p = 1.8 mm), which is at a low level. Most of the air passes through the middle of two adjacent fins, and the air cannot effectively scour the slit fin, resulting in the small h and Δp. As the slotted height continues to increase to about half of the fin pitch (S_h / F_p = 0.5), the slit is roughly the same distance from the upper layer and the lower layer fins. Further, the incoming air can form an effective scour and have the largest turbulence intensity in the channel between the two layers of fins, resulting in the largest h and Δp. As the slotted height further increases to 0.9 mm (F_p = 1.2 mm) or 1.6 mm (F_p = 1.8 mm), the slit begins to approach the upper fin. The channel between the upper and lower fins becomes larger, in which most of the air passes through. The air cannot effectively scour the slit fin, indicating that the h and Δp begin to decrease. Fig. 10 shows the temperature distributions of slit fins at y = 2 mm. If the slotted height is too large or too small, there will be situations where the air cannot be effectively heated. As the slotted height is about half of the fin pitch (S_h / F_p = 0.5), the air can effectively scour the fins, and the area of the low temperature region along the flow direction is the smallest.

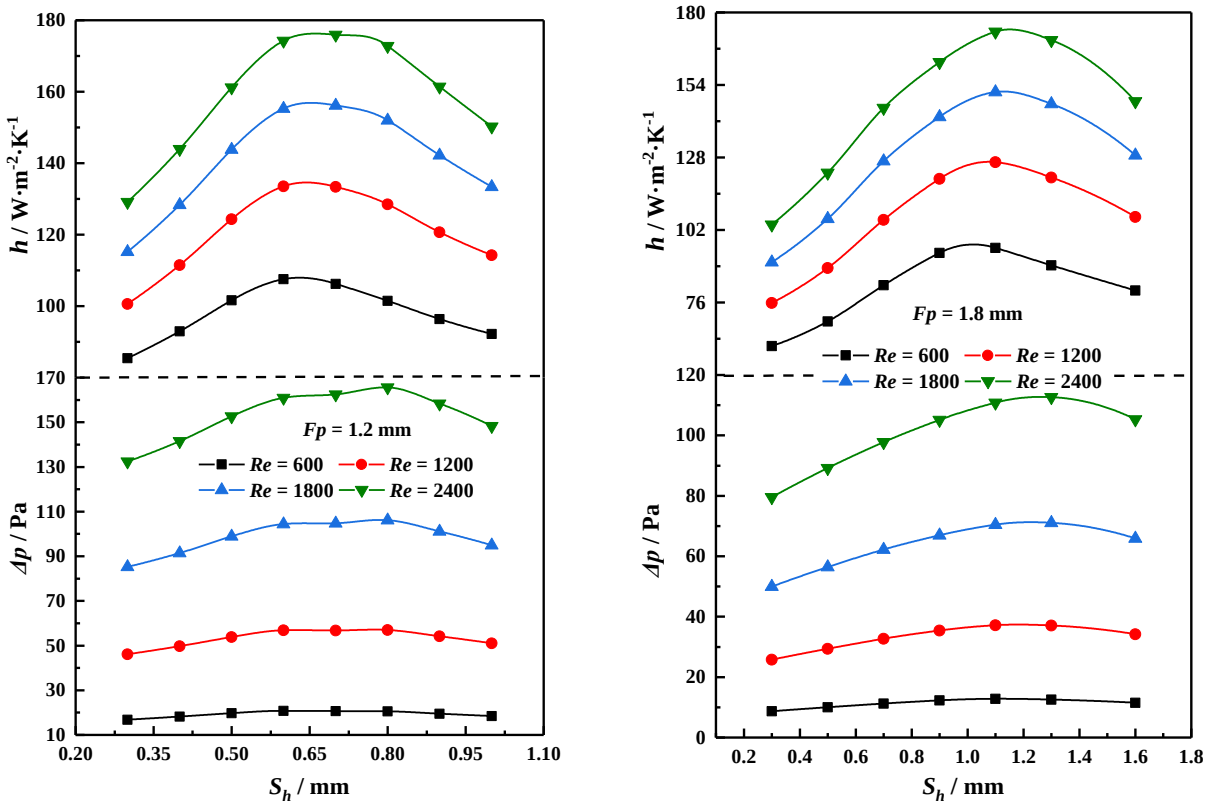

(a) Fp = 1.2 mm *(b) Fp = 1.8 mm*

Figure 8. Effects of slotted height on h and Δp at different fin pitches for slit fin

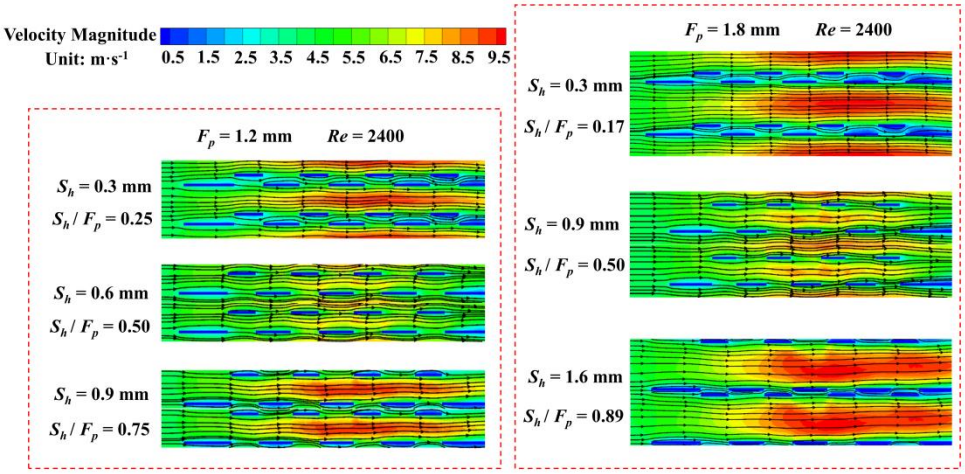

Figure 9. Contours of velocity and streamline at different slotted heights (y = 2.0 mm)

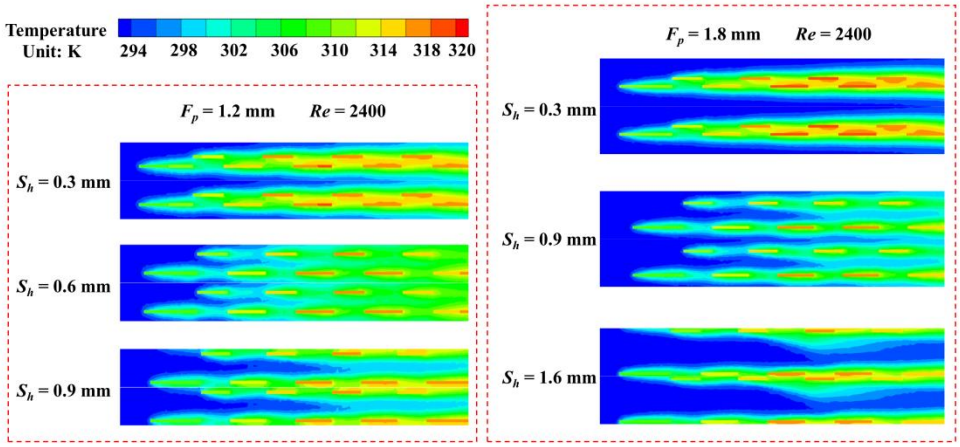

Figure 10. Contours of temperature at different slotted heights and fin pitches (y = 2.0 mm)

3.3. The effect of slotted height on *PEC*

Fig. 11 demonstrates the comprehensive performance for louver fin and slit fin at different fin pitches. First of all, it can be concluded that under different Reynolds numbers, the trend of the *PEC* with the slotted height is consistent with the trend of the above heat transfer coefficient on the whole. And with the increasing Reynolds number, the *PEC* under the same condition decreases, which is mainly due to the faster increase of the flow resistance compared with the heat transfer coefficient with the increasing Reynolds number. Secondly, as the slotted height is about 0.3~0.45 times of the fin pitch, the *PEC* of the louver fin can reach the maximum. And the maximum *PEC* under 1.2 mm fin pitch is greater than the maximum *PEC* under 1.8 mm fin pitch. For the slit fin, as the slotted height is about 0.5~0.65 times of the fin pitch, the *PEC* reaches the maximum. With the increasing Reynolds number, the optimal slotted height will increase slightly. It is different from the louver fin that the maximum *PEC* under 1.2 mm fin pitch is less than the maximum *PEC* under 1.8 mm fin pitch. Meanwhile, it can be seen that as the fin pitch is 1.2 mm, the *PEC* of louver fin at different Reynolds numbers is greater than that of slit fin, indicating that the benefit of heat transfer coefficient brought by the change of flow direction is greater than the cost of increasing flow resistance. However, as the fin pitch is 1.8 mm and the slotted height is large, the *PEC* of the louver fin is roughly equivalent to that

of the slit fin, which indicates that the increase rate of heat transfer coefficient caused by the change of flow direction is roughly equal to the increase rate of flow resistance.

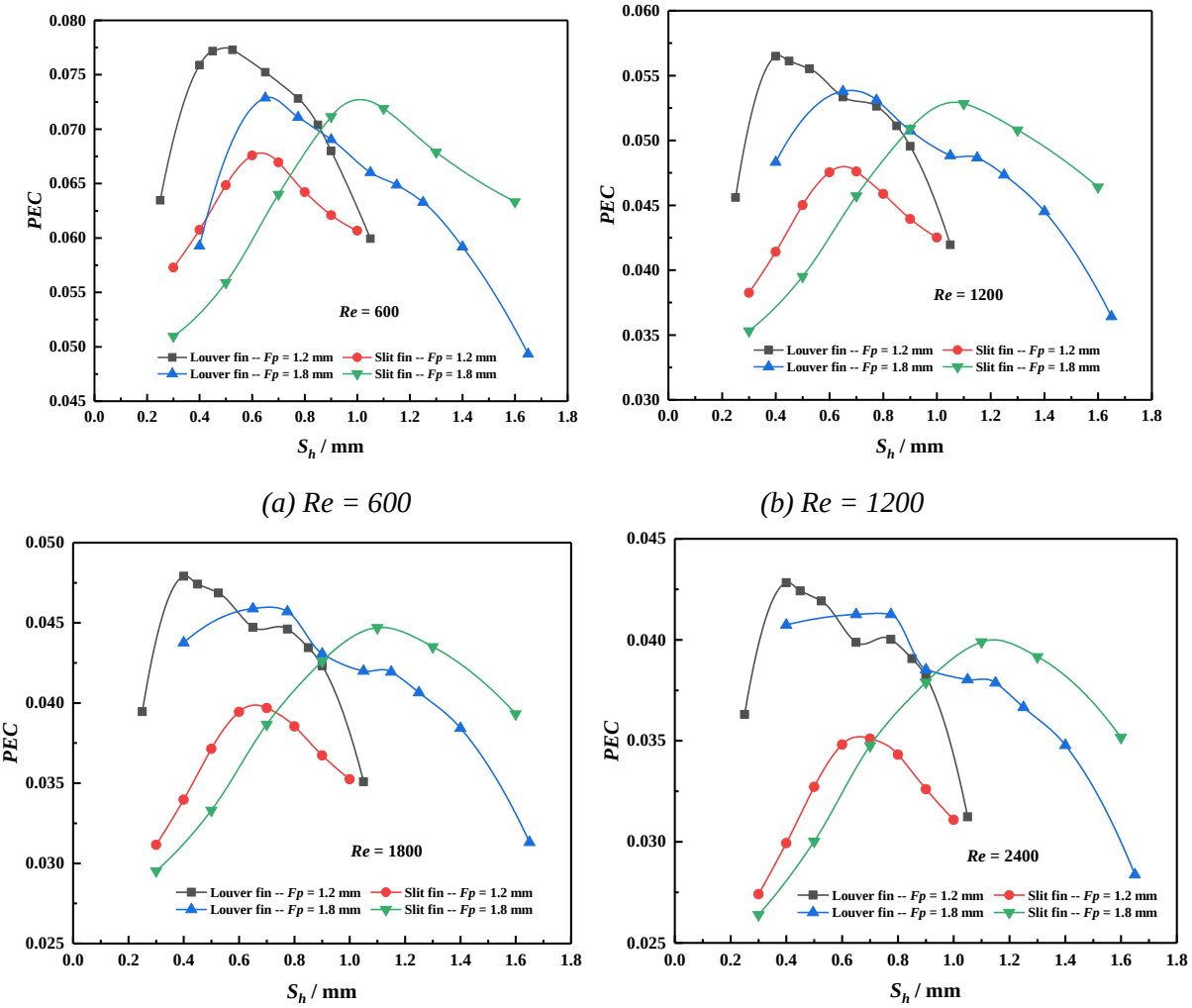

(a) Re = 600 *(b) Re = 1200*

(a) Re = 1800 *(b) Re = 2400*

Figure 11. Varieties in *PEC* with the increasing slotted height at different Reynolds numbers

4. Conclusions

The optimal angle or slotted height is different under different fin pitches, and there is no criterion to link the louver angle or slotted height with fin pitch in current research. Therefore, this paper tries to define the slotted height of the louver fin according to the meaning of the slotted height of the slit fin, and explores the interaction function between the slotted height and the fin pitch. Combined with the distributions of velocity and streamline, the effects of slotted height on air side performance at different fin pitches for louver fin and slit fin are investigated in detail. The main conclusions are summarized as follows.

(1) With the increasing slotted height for louver fin, the overall trend of the heat transfer coefficient at low Reynolds number is to increase first and then decrease. In the cases of high Reynolds number, the “bimodal phenomenon” begins to appear. As the slotted height is about half of the fin pitch, the heat transfer coefficient has a local minimum value, of which there are two peaks on

both sides. However, the pressure drop has been increasing with the increase of the slotted height. According to the geometric relationship, it can be found that the optimal slotted height under different fin pitches is more instructive than the optimal louver angle.

(2) In the cases of slit fin, the heat transfer coefficient and pressure drop increase first and then decrease with the increasing slotted height. As the slotted height is half of the fin pitch, the heat transfer coefficient and pressure drop can reach a maximum. And with the increase of Reynolds number, the slotted height corresponding to the maximum value increases.

(3) The comprehensive performance of louver fin and slit fin at different Reynolds numbers is compared. As the slotted height is about 0.3~0.45 times and 0.5~0.65 times of fin pitch for louver fin and slit fin respectively, the comprehensive performance can reach a maximum. The maximum *PEC* under 1.2 mm fin pitch is greater than the maximum *PEC* under 1.8 mm fin pitch. It is different from the louver fin that the maximum *PEC* under 1.2 mm fin pitch is less than the maximum *PEC* under 1.8 mm fin pitch. In general, louver fin has higher comprehensive performance than slit fin. However, for the fin pitch assigned to 1.8 mm and large slotted height, the louver fin has a comprehensive performance roughly similar to the slit fin.

Nomenclature

Do	tube outside diameter [m]	c_p	specific heat [Jkg-1K-1]
Dc	Collar diameter [m]	m	mass flow rate [kgs-1]
Ac	minimal flow area [m2]	h	heat transfer coefficient [WK-1m-2]
Ao	total surface area [m2]	Q	heat transfer rate [W]
A_{total}	total heat transfer area [m2]	***Greek symbols***	
Pt	transverse tube pitch [m]		
Pl	longitudinal tube pitch [m]	λ	thermal conductivity [Wm-1K-1]
N	number of tube rows	ρ	density [kgm-3]
Fp	fin pitch [m]	μ	dynamic viscosity [Pas]
S_h	slotted height [m]	η	fin efficiency
δ_f	fin thickness [m]	Δp	pressure drop [Pa]
Nu	Nusselt number	ΔT_{log}	Log mean temperature difference [K]
f	Friction factor	***Subscript***	
Re	Reynolds number	in	inlet
T	temperature [K]	out	outlet
p	pressure [Pa]	max	maximum
u	velocity [ms-1]	w	wall

Acknowledgements

This work is supported by National Natural Science Foundation of China (Nos. 52006164 and 52276019) and Fundamental Research Funds for the Central Universities (No. xzy012022074).

References

[1] Sahoo, R.R., *et al.*, Performance comparison of various coolants for louvered fin tube automotive radiator, *Thermal Science*, *21* (2017), 6 Part B, pp. 2871-2881, DOI No. https://doi.org/10.2298/TSCI150219213S

[2] Kong, Y.Q., *et al.*, Effects of continuous and alternant rectangular slots on thermo-flow performances of plain finned tube bundles in in-line and staggered configurations, *International Journal of Heat and Mass Transfer*, *93* (2016), pp. 97-107, DOI No. https://doi.org/10.1016/j.ijheatmasstransfer.2015.10.008

[3] Sadeghianjahromi, A., Wang, C.-C., Heat transfer enhancement in fin-and-tube heat exchangers – A review on different mechanisms, *Renewable and Sustainable Energy Reviews*, *137* (2021), p. 110470, DOI No. https://doi.org/10.1016/j.rser.2020.110470

[4] Chu, H., *et al.*, Progress in enhanced pool boiling heat transfer on macro- and micro-structured surfaces, *International Journal of Heat and Mass Transfer*, *200* (2023), p. 123530, DOI No. https://doi.org/10.1016/j.ijheatmasstransfer.2022.123530

[5] Jiang, H., *et al.*, Effect of T-shaped micro-fins on pool boiling heat transfer performance of surfaces, *Experimental Thermal and Fluid Science*, *136* (2022), p. 110663, DOI No. https://doi.org/10.1016/j.expthermflusci.2022.110663

[6] Kays, W., London, A., Heat-Transfer and Flow-Friction Characteristics of Some Compact Heat-Exchanger Surfaces: Part 1—Test System and Procedure, *Transactions of the American Society of Mechanical Engineers*, *72* (1950), 8, pp. 1075-1085, DOI No. https://doi.org/10.1115/1.4016920

[7] Kim, M.-H., Bullard, C.W., Air-side thermal hydraulic performance of multi-louvered fin aluminum heat exchangers, *International Journal of Refrigeration*, *25* (2002), 3, pp. 390-400, DOI No. https://doi.org/10.1016/S0140-7007(01)00025-1

[8] Qi, Z.-G., *et al.*, Parametric study on the performance of a heat exchanger with corrugated louvered fins, *Applied Thermal Engineering*, *27* (2007), 2, pp. 539-544, DOI No. https://doi.org/10.1016/j.applthermaleng.2006.06.015

[9] Hsieh, C.-T., Jang, J.-Y., Parametric study and optimization of louver finned-tube heat exchangers by Taguchi method, *Applied Thermal Engineering*, *42* (2012), pp. 101-110, DOI No. https://doi.org/10.1016/j.applthermaleng.2012.03.003

[10] Erbay, L.B., *et al.*, Numerical investigation of the air-side thermal hydraulic performance of a louvered-fin and flat-tube heat exchanger at low Reynolds numbers, *Heat Transfer Engineering*, *38* (2017), 6, pp. 627-640, DOI No. https://doi.org/10.1080/01457632.2016.1200382

[11] Javaherdeh, K., *et al.*, Experimental and numerical investigations on louvered fin-and-tube heat exchanger with variable geometrical parameters, *Journal of Thermal Science and Engineering Applications*, *9* (2017), 2, DOI No. https://doi.org/10.1115/1.4035449

[12] Qian, Z., *et al.*, Simulation investigation on inlet velocity profile and configuration parameters of louver fin, *Applied Thermal Engineering*, *138* (2018), pp. 173-182, DOI No. https://doi.org/10.1016/j.applthermaleng.2018.02.009

[13] Sadeghianjahromi, A., *et al.*, Optimization of the louver fin-and-tube heat exchangers− A parametric approach, *Journal of Enhanced Heat Transfer*, *27* (2020), 4, DOI No. https://10.1615/JEnhHeatTransf.2020033527

[14] Nakayama, W., Xu, L., *Enhanced fins for air-cooled heat exchangers—heat transfer and friction*

correlations,1st ASME/JSME Thermal Engineering Joint Conference, New York, USA,1983,1, pp. 495-502
[15] Garimella, S., *et al.*, Tube and Fin Geometry Alternatives for the Design of Absorption-Heat-Pump Heat Exchangers, *4* (1997), 3, pp. 217-235, DOI No. https://10.1615/JEnhHeatTransf.v4.i3.50
[16] Wang, C.-C., *et al.*, An investigation of the airside performance of the slit fin-and-tube heat exchangers, *International Journal of Refrigeration*, *22* (1999), 8, pp. 595-603, DOI No. https://doi.org/10.1016/S0140-7007(99)00031-6
[17] Du, Y.-J., Wang, C.-C., An experimental study of the airside performance of the superslit fin-and-tube heat exchangers, *International Journal of Heat and Mass Transfer*, *43* (2000), 24, pp. 4475-4482, DOI No. https://doi.org/10.1016/S0017-9310(00)00082-X
[18] Wang, C.-C., *et al.*, A comparative study of compact enhanced fin-and-tube heat exchangers, *International Journal of Heat and Mass Transfer*, *44* (2001), 18, pp. 3565-3573, DOI No. https://doi.org/10.1016/S0017-9310(01)00011-4
[19] Yun, J.-Y., Lee, K.-S., Influence of design parameters on the heat transfer and flow friction characteristics of the heat exchanger with slit fins, *International Journal of Heat and Mass Transfer*, *43* (2000), 14, pp. 2529-2539, DOI No. https://doi.org/10.1016/S0017-9310(99)00342-7
[20] Wang, Z., Ouyang, X., Numerical simulation of heat transfer and flow characteristics for plate fin-and-tube heat exchanger with ring-bridge slit fins, *Thermal Science*, 2023, OnLine-First, DOI No. https://doi.org/10.2298/TSCI230123096W
[21] Zhi, C., *et al.*, Numerical investigation of slit fin at different Reynolds numbers: A sensitivity analysis and optimization by Taguchi methodology, *International Communications in Heat and Mass Transfer*, *138* (2022), p. 106393, DOI No. https://doi.org/10.1016/j.icheatmasstransfer.2022.106393
[22] Zhi, C., *et al.*, Prediction and analysis of thermal-hydraulic performance with slit fins in small diameter (3 mm to 4 mm) heat exchangers, *International Communications in Heat and Mass Transfer*, *129* (2021), p. 105684, DOI No. https://doi.org/10.1016/j.icheatmasstransfer.2021.105684
[23] Li, J., *et al.*, Numerical study on a slit fin-and-tube heat exchanger with longitudinal vortex generators, *International Journal of Heat and Mass Transfer*, *54* (2011), 9, pp. 1743-1751, DOI No. https://doi.org/10.1016/j.ijheatmasstransfer.2011.01.017
[24] Moreno, R.R., *et al.*, Numerical optimization of a heat exchanger with slit fins and vortex generators using genetic algorithms, *International Journal of Refrigeration*, *119* (2020), pp. 247-256, DOI No. https://doi.org/10.1016/j.ijrefrig.2020.07.023
[25] Zhang, X., *et al.*, Numerical investigation of the air-side performance of louver fin-and-tube radiators having rectangular, tapered and airfoil section configuration, *Energy Reports*, *8* (2022), pp. 11799-11809, DOI No. https://doi.org/10.1016/j.egyr.2022.09.050
[26] Menéndez Pérez, A., *et al.*, Parametric analysis of the influence of geometric variables of vortex generators on compact louver fin heat exchangers, *Thermal Science and Engineering Progress*, *27* (2022), p. 101151, DOI No. https://doi.org/10.1016/j.tsep.2021.101151
[27] Yoo, B.K., *et al.*, Numerical analysis and correlation of thermohydraulic characteristics of louvered fin-tube heat exchanger, *International Journal of Refrigeration*, (2022), DOI No. https://doi.org/10.1016/j.ijrefrig.2022.08.021

[28] Li, X.-Y., *et al.*, Numerical study on the heat transfer and pressure drop characteristics of fin-and-tube surface with four round-convex strips around each tube, *International Journal of Heat and Mass Transfer*, *158* (2020), p. 120034, DOI No. https://doi.org/10.1016/j.ijheatmasstransfer.2020.120034
[29] Roache, P.J., Perspective: A Method for Uniform Reporting of Grid Refinement Studies, *Journal of Fluids Engineering*, *116* (1994), 3, pp. 405-413, DOI No. https://doi.org/10.1115/1.2910291
[30] Naik, H., Tiwari, S., Thermal performance analysis of fin-tube heat exchanger with staggered tube arrangement in presence of rectangular winglet pairs, *International Journal of Thermal Sciences*, *161* (2021), p. 106723, DOI No. https://doi.org/10.1016/j.ijthermalsci.2020.106723
[31] Eça, L., Hoekstra, M., Evaluation of numerical error estimation based on grid refinement studies with the method of the manufactured solutions, *Computers & Fluids*, *38* (2009), 8, pp. 1580-1591, DOI No. https://doi.org/10.1016/j.compfluid.2009.01.003
[32] Saleem, A., Kim, M.-H., Airside thermal performance of louvered fin flat-tube heat exchangers with different redirection louvers, *Energies*, *15* (2022), 16, p. 5904, DOI No. https://doi.org/10.3390/en15165904
[33] Zhi, C., *et al.*, Thermodynamic assessment and optimization on louver fin with non-uniform arrangement at different tube rows by desirability approach, *Thermal Science and Engineering Progress*, *42* (2023), p. 101899, DOI No. https://doi.org/10.1016/j.tsep.2023.101899
[34] Perrotin, T., Clodic, D., Thermal-hydraulic CFD study in louvered fin-and-flat-tube heat exchangers, *International Journal of Refrigeration*, *27* (2004), 4, pp. 422-432, DOI No. https://doi.org/10.1016/j.ijrefrig.2003.11.005
[35] Čarija, Z., *et al.*, Heat transfer analysis of fin-and-tube heat exchangers with flat and louvered fin geometries, *International journal of refrigeration*, *45* (2014), pp. 160-167, DOI No. https://doi.org/10.1016/j.ijrefrig.2014.05.026
[36] Wang, C.-C., *et al.*, Heat transfer and friction correlation for compact louvered fin-and-tube heat exchangers, *International journal of heat and mass transfer*, *42* (1999), 11, pp. 1945-1956, DOI No. https://doi.org/10.1016/S0017-9310(98)00302-0

Received: 27.03.2023.
Revised: 03.06.2023.
Accepted: 14.06.2023.